



Published in final edited form as:

*J Biomed Mater Res B Appl Biomater*. 2012 February ; 100(2): 569–576. doi:10.1002/jbm.b.31987.

## Synthesis and evaluation of novel dental monomer with branched aromatic carboxylic acid group

Jonggu Park<sup>1</sup>, Qiang Ye<sup>1</sup>, Viraj Singh<sup>2</sup>, Sarah L. Kieweg<sup>2</sup>, Anil Misra<sup>1,3</sup>, and Paulette Spencer<sup>1,2</sup>

<sup>1</sup>Bioengineering Research Center, School of Engineering, University of Kansas, Lawrence, Kansas

<sup>2</sup>Department of Mechanical Engineering, University of Kansas, Lawrence, Kansas

<sup>3</sup>Department of Civil, Environmental, and Architectural Engineering, University of Kansas, Lawrence, Kansas

### Abstract

A new glycerol-based dimethacrylate monomer with an aromatic carboxylic acid, 2-((1,3-bis(methacryloyloxy)propan-2-yloxy)carbonyl)benzoic acid (BMPB), was synthesized, characterized, and proposed as a possible dental co-monomer for dentin adhesives. Dentin adhesives containing 2-hydroxyethyl methacrylate (HEMA) and 2,2-bis[4-(2-hydroxy-3-methacryloxypropoxy) phenyl]propane (BisGMA) in addition to BMPB were formulated with water at 0, 5, 10, and 15 wt % to simulate wet, oral conditions, and photo-polymerized. Adhesives were characterized with regard to viscosity, real-time photopolymerization behavior, dynamic mechanical analysis, and microscale 3D internal morphologies and compared with HEMA/BisGMA controls. When formulated under wet conditions, the experimental adhesives showed lower viscosities (0.04–0.07 Pa s) as compared to the control (0.09–0.12 Pa s). The experimental adhesives showed higher glass transition temperature (146–157°C), degree of conversion (78–89%), and rubbery moduli (33–36 MPa), and improved water miscibility (no voids) as compared to the controls (123–135°C, 67–71%, 15–26 MPa, and voids, respectively). The enhanced properties of these adhesives suggest that BMPB with simple, straight-forward synthesis is a promising photocurable co-monomer for dental restorative materials.

### Keywords

dentin adhesives; dental monomer; photopolymerization; dynamic mechanical property; water miscibility

## INTRODUCTION

After nearly five decades of research, dental composites continue to show limited clinical service, requiring replacement at 5.7 years because of secondary decay or fracture.<sup>1</sup> Clinical observations suggest that the incidence of decay is increased at the margins of composite

restorations and the gingival margin is a particularly vulnerable site.<sup>2,3</sup> The composite is too viscous to bond directly to the tooth and thus, a low viscosity adhesive must be used to form a bond between the tooth and composite.

Acid-etching provides effective mechanical bonding between enamel and adhesive, but bonding to dentin has been fraught with problems. Clinicians frequently find very little enamel available for bonding at the gingival margin of class II composite restorations and thus, the bond at this margin depends on the integrity of the adhesive seal formed with dentin.<sup>4</sup> At the vulnerable gingival margin, the adhesive may serve as the primary barrier between the prepared tooth and the surrounding environment. A failed adhesive means that there are gaps between the tooth and composite. Bacterial enzymes, oral fluids, and bacteria can infiltrate these gaps; this activity will lead to recurrent decay, hypersensitivity, pulpal inflammation, and restoration failure.<sup>5-7</sup>

Water present in the mouth is a major interfering factor when bonding adhesives and/or composites to the tooth.<sup>8</sup> Water content of the dentin surface varies as a function of depth,<sup>9</sup> the nature of the substrate (i.e., caries-affected or healthy dentin),<sup>10</sup> and the presence of residual rinse water. Under *in vivo* conditions, there is little control over the amount of water left on the tooth during dentin bonding. It is possible to leave the dentin surface so wet that the adhesive resin undergoes physical separation into hydrophilic and hydrophobic-rich phases.<sup>11</sup> Adhesive phase separation inhibits the formation of an impervious, structurally integrated bond at the composite/tooth interface.<sup>12,13</sup> *In vitro* and *in vivo* studies have suggested that the factors that inhibit a durable adhesive/dentin bond include inadequate monomer/polymer conversion, adhesive phase separation, hydrolytic, and enzymatic degradation.<sup>8,11,14</sup> We are addressing these factors by developing water-compatible methacrylate-based dentin adhesives.<sup>11-13,15-22</sup>

The selection of the monomers used in dentin adhesives is a particularly critical factor since polymerization of the resin monomers produces a crosslinked matrix that provides chemical/thermal stability and mechanical strength. Monomer selection exerts considerable influence on the properties, durability, and behavior of dentin adhesives in the wet, oral environment. Although numerous monomers have been investigated,<sup>18,23-25</sup> the lack of dentin adhesives that are both effective and durable continues to be a major problem with the use of composites in direct restorative dentistry.

The durability of the adhesive/dentin bond is closely related to the water miscibility and appropriate photopolymerization of adhesive resins in the presence of water. In this work, a new glycerol-based dimethacrylate with an aromatic carboxylic acid is proposed as a dental monomer that will provide improved water miscibility, dynamic mechanical properties, and increased monomer/polymer conversion. The objective of this study was to synthesize and characterize a new dimethacrylate monomer and to evaluate the properties of the dentin adhesive formulated with the newly synthesized monomer under conditions that simulate the wet, oral environment.

## MATERIAL AND METHODS

### Materials

2,2-Bis[4-(2-hydroxy-3-methacryloxypropoxy) phenyl]propane (BisGMA, Polysciences, Warrington, PA) and 2-hydroxyethylmethacrylate (HEMA, Acros Organics, NJ) were used as received without further purification as monomers in dentin adhesives. 2-((1,3-Bis(methacryloyloxy)propan-2-yloxy)carbonyl)benzoic acid (BMPB) was used as a co-monomer and synthesized in-house (Figure 1). The phthalic anhydride and 4-(dimethylamino)pyridine were obtained from Acros Organics (NJ). Glycerol dimethacrylate was obtained from Sigma-Aldrich (St. Louis, MO). Camphoroquinone (CQ) and ethyl-4-(dimethylamino)benzoate (EDMAB) were obtained from Sigma-Aldrich (St. Louis, MO). All other chemicals were reagent grade and used without further purification.

### Monomer synthesis (BMPB)

The new monomer, BMPB, was synthesized following the procedures described by Catel et al., with slight modification.<sup>26,27</sup> Briefly, phthalic anhydride (PA, 0.068 mol) was dissolved in tetrahydrofuran (THF, 50 mL) at room temperature. 4-(Dimethylamino)pyridine (DMAP, 0.003 mol) was added to the reaction mixture, followed by dropwise addition of glycerol dimethacrylate (GDMA, 0.075 mol). Following complete addition of GDMA, the reaction was allowed to continue at 60°C for another 3 h under nitrogen atmosphere. The reaction was monitored by thin layer chromatography (mobile phase: CH<sub>2</sub>Cl<sub>2</sub>:MeOH = 5:1). After the reaction was completed, the mixture was quenched with cold water and extracted with ethyl acetate. The organic phase was washed twice with a solution of 1N HCl to remove DMAP and extracted with 0.5M NaHCO<sub>3</sub>. The aqueous basic layer was acidified to pH 1–2 with 1N HCl and then extracted with ethyl acetate. After drying over anhydrous MgSO<sub>4</sub>, 0.05 wt % of 2,6-di-*tert*-butyl-4-methylphenol (BHT) was added and the solvent removed with a rotary evaporator at 35–40°C to obtain BMPB as a colorless oil (18.9 g, 74% yield). The scheme for the BMPB synthesis is shown in Figure 1. The structure of this synthesized compound (BMPB) was confirmed using FTIR (Spectrum 400, Perkin-Elmer, Waltham, MA), <sup>1</sup>H NMR, and <sup>13</sup>C NMR (FT-400 MHz Bruker Spectrometer, DMSO as solvent) spectroscopy.

### Preparation of adhesive formulations

The experimental adhesive formulations consisted of HEMA, BisGMA, and BMPB with a mass ratio of 45/30/25, in which BMPB was used as a co-monomer. The experimental adhesives were formulated with 0 (E0), 5 (E5), 10 (E10), and 15 wt % (E15) water to simulate the moist environment of the mouth. Control adhesive formulations with HEMA/BisGMA = 45/55 w/w ratio, which is similar to commercial dentin adhesives, were also formulated with 0 (C0), 5 (C5), 10 (E10), and 15 wt % (C15) water. CQ (0.5 wt %) and EDMAB (0.5 wt %) were used as photoinitiator and co-initiator, respectively, with respect to the total amount of monomer. Mixtures of monomers/photoinitiators were prepared in a brown glass vial in the absence of visible light. The solutions containing the monomers/photoinitiators were mixed overnight at room temperature to promote complete dissolution and formation of a homogeneous solution. The prepared resins were injected into a glass-tubing mold (Fiber Optic Center, Inc., part no.: ST8100, New Bedford, MA) and light-cured

for 40 s at room temperature with a LED light curing unit (LED Curebox, Proto-tech, Portland, OR). The polymerized samples were stored in the dark at room temperature for 48 h and 1 week in a vacuum oven in the presence of a drying agent at 37°C. The resultant rectangular beam specimens (1 × 1 × 15 mm<sup>3</sup>) were used to determine the dynamic mechanical properties and microscale morphologies.

### Viscosities of the adhesive resins

Rheological measurements for the liquid resin formulated with/without water were carried out in a TA Instruments AR2000 rheometer (New Castle, DE) in the controlled-rate mode. The measurements were made at 25°C with 40 mm diameter and 2° cone angle in the shear rate range of 10/s to 100/s, at 10 points per decade to generate data on viscosity and shear rate.

### Real-time double bond conversion and maximal polymerization rate

Real-time *in situ* monitoring of the photopolymerization of the different adhesive solutions was performed using an infrared spectrometer (Spectrum 400 Fourier transform infrared spectrophotometer, Perkin-Elmer, Waltham, MA) at a resolution of 4 cm<sup>-1</sup>.<sup>18</sup> One drop of adhesive solution was placed on the diamond crystal top plate of an attenuated total reflectance (ATR) accessory (PIKE Technologies Gladi-ATR, Madison, WI) and covered with a mylar film to prevent oxygen inhibition of polymerization. A 40-s-exposure to the commercial visible-light-polymerization unit (Spectrum<sup>®</sup> 800, Dentsply, Milford, DE) at an intensity of 550 mW cm<sup>-2</sup> was initiated after 50 spectra had been recorded. Real-time IR spectra were continuously recorded for 600 s after light activation began. A time-based spectrum collector (Spectrum TimeBase, Perkin-Elmer) was used for continuous and automatic collection of spectra during polymerization. Three replicates were obtained for each adhesive formulation. The change of the band ratio profile (1637 cm<sup>-1</sup> (C = C)/1608 cm<sup>-1</sup> (phenyl) was monitored and degree of conversion (DC) was calculated using the following equation based on the decrease in the absorption intensity band ratio before and after light curing.

$$DC = \left(1 - \frac{\text{Absorbance}_{1637\text{cm}^{-1}}^{\text{sample}} / \text{Absorbance}_{16308\text{cm}^{-1}}^{\text{sample}}}{\text{Absorbance}_{1637\text{cm}^{-1}}^{\text{monomer}} / \text{Absorbance}_{1608\text{cm}^{-1}}^{\text{monomer}}}\right) \times 100\%$$

The average of the last 50 of time-based spectra is reported as the DC value. The maximal polymerization rate ( $R_{\text{max}}$ ) was determined using the maximum slope of the linear region of the DC-time plots.<sup>28</sup> For all experimental groups, the differences between DC or polymerization rate were analyzed using analysis of variance (ANOVA), together with Tukey's test at  $\alpha = 0.05$  (Microcal Origin Version 6.0, Microcal Software Inc., Northampton, MA).

### Micro-X-ray tomography

The microscale morphologies of rectangular beam specimens cured in the presence of 11 wt % water were observed using three-dimensional (3D) Micro X-ray Computer Tomography (MicroXCT-400, Xradia Inc. Concord, CA). Computer tomography (CT) facilitates viewing

of an object in 3D and allows selection of virtual slices spaced by 1  $\mu\text{m}$ , thus illustrating the bulk structure of heterogeneous materials. The transmission X-ray imaging of the samples was performed using an X-ray tube with a tungsten anode setting of 50 kV at 6 W with an optical magnification of  $\times 20$ . The 3D images were constructed with the help of software “XM Reconstructor 8.0” using 2160 images taken at 15 s exposure time per image.

### Dynamic mechanical analysis

Dynamic mechanical analysis (DMA) is a thermal analysis technique that measures the properties of materials as they are deformed under periodic stress. In this study, DMA tests were performed using a TA instruments Q800 (TA Instruments, New Castle, USA) with a three-point bending clamp. The dynamic mechanical properties determined by DMA have been described previously.<sup>29</sup> A sinusoidal stress is applied and the resultant strain is measured. The properties measured under this oscillating loading are storage modulus, loss modulus, and  $\tan \delta$ . The storage modulus ( $E'$ ) represents the stiffness of a viscoelastic material and is proportional to the energy stored during a loading cycle. The loss modulus ( $E''$ ) is related to the amount of energy lost due to viscous flow. The ratio of loss ( $E''$ ) to storage modulus ( $E'$ ) is referred to as the mechanical damping, or  $\tan \delta$ . The test temperature was varied from 0 to 200°C with a ramping rate of 3 °C  $\text{min}^{-1}$  at a frequency of 1 Hz. The storage modulus and  $\tan \delta$  were recorded as a function of temperature. The  $\tan \delta$  value goes through a maximum as the polymer undergoes the transition from the glassy to the rubbery state. The glass transition temperature ( $T_g$ ) was determined as the position of the maximum on the  $\tan \delta$  versus temperature plot. Rectangular beam specimens (1  $\times$  1  $\times$  15  $\text{mm}^3$ ) prepared as described previously were used for DMA measurements. Five specimens of each material were measured. The results were analyzed statistically using analysis of variance (ANOVA), together with Tukey’s test at  $\alpha = 0.05$  (Microcal Origin Version 6.0, Microcal Software Inc., North-ampton, MA).

## RESULTS

The structure of the newly synthesized dimethacrylate monomer (BMPB) was identified using FTIR,  $^1\text{H}$  NMR, and  $^{13}\text{C}$  NMR (FT-400 MHz Bruker Spectrometer, DMSO as solvent) spectroscopy. The characteristic FTIR peaks for BMPB are: 3400–3400  $\text{cm}^{-1}$  (OH stretching for  $-\text{COOH}$ ), 1722  $\text{cm}^{-1}$  (C=O stretching), 1637  $\text{cm}^{-1}$  (C=CH bending on methacrylate group), 1285, 1256, and 1157  $\text{cm}^{-1}$  (C=O stretching), and 814  $\text{cm}^{-1}$  (C=C twisting). Disappearance of the anhydride peak at 1849 and 1760  $\text{cm}^{-1}$  and appearance of the C=C stretching band at 1637  $\text{cm}^{-1}$  confirmed the formation of the new dimethacrylate monomer. Figure 2(A,B) present correspondingly the  $^1\text{H}$  NMR and  $^{13}\text{C}$  NMR spectra of BMPB. In the  $^1\text{H}$  NMR spectrum [Figure 2(A); DMSO- $d_6$ , 400 MHz], the chemical shifts of BMPB were (ppm): (a) 1.9 (6H,  $-\text{CH}_3$ ); (b) 4.4 (4H,  $-\text{CH}_2\text{O}$ ); (c) 5.6 (1H,  $-\text{CH}$ ); (d) 6.1, 5.7 (4H,  $=\text{CH}_2$  *trans, cis*); (e) 7.5, 7.8 (4H, Ar); (f) 13.3 (1H,  $-\text{COOH}$ ). In the  $^{13}\text{C}$  NMR [Figure 2(B); DMSO- $d_6$ ]:  $\delta$  (ppm) = (a) 16.1 (C=C- $\underline{\text{C}}\text{H}_3$ ); (b) 60.4 (O $\underline{\text{C}}\text{H}_2$ -CH); (c) 67.9 ( $\underline{\text{C}}\text{H}-\text{CH}_2$ ); (d) 124.6 ( $\underline{\text{C}}\text{H}_2=\text{C}$ ); (f) 126.4, 127.2, 129.5, 130.1 (Ar); (e) 133.5 ( $\text{CH}_2=\underline{\text{C}}$ ); 164.0, 164.3, 165.0, 165.4, 166.0 (C=O, esters and acid).

Figure 3 shows the viscosities of control [Figure 3(A)] and experimental resins [Figure 3(B)] with different water concentration as a function of shear rate at 25°C. The viscosity of the resin solutions decreased in the order (Pa s): C0 (0.19) > E0  $\cong$  C5 (0.12) > C10  $\cong$  C15 (0.09) > E5 (0.07) > E10 (0.05) > E15 (0.04).

Real-time photopolymerization kinetic behavior of the control and experimental adhesives is shown in Figure 4. It can be seen that the addition of water has a dramatic effect on the DC. With increasing water content, DC varied from 61 to 71% for the control [Figure 4(A)] and from 67 to 89% for the experimental [Figure 4(B)]. At each level of water content, the DC of the experimental adhesives was significantly higher than that of the control ( $p < 0.05$ ). No obvious change in DC was observed after 60 s (Figure 4). Comparison of the plots in Figure 5 revealed different photopolymerization kinetics with the inclusion of the new monomer, BMPB, and the presence of water. The maximal polymerization rates of control and experimental adhesives as a function of water are shown in Figure 5. For all the adhesives, maximal polymerization rates decreased with the increase in water content (0–15 wt %): from  $0.06 \pm 0.01$  to  $0.03 \pm 0.01$  for the control; from  $0.08 \pm 0.01$  to  $0.06 \pm 0.01$  for the experimental adhesives. At each level of water content, the polymerization rates of the experimental adhesives were significantly higher than those of the control ( $p < 0.05$ ).

The dynamic mechanical properties of dentin adhesive polymers cured in the absence or presence of water were measured by 3-point bending clamp at various temperatures and summarized in Table I. The storage modulus values at 37°C for both the experimental and control adhesives decreased with increasing water content. The experimental adhesives cured in the presence of water (E5, E10, E15) showed higher storage moduli at 37°C, rubbery moduli, and  $T_g$ s than the corresponding controls (C5, C10, C15). In the rubbery region, the average storage moduli of experimental adhesives cured in the presence of water were in the range of 33–36 MPa, which were significantly greater ( $p < 0.05$ ) than those of the control adhesives (15–26 MPa).  $T_g$  values for C0 and E0 were nearly identical (144–145°C), but there were significant differences ( $p < 0.05$ ) in  $T_g$  between the control and experimental adhesives cured in the presence of water. In addition, the tan  $\delta$  peak heights (0.62–0.65) of the experimental adhesives were lower than those of control adhesives (0.67–0.79). The full-width-at-half-maximum values of tan  $\delta$  for all samples tested were in the range of 33–49, showing a wide range of widths of the tan  $\delta$  curves.

The internal morphology of the control and experimental adhesive polymers are shown in Figure 6. The voids in the control sample (A) indicate microphase separation when the control adhesive is polymerized in the presence of 11 wt % water. In comparison, no voids are observed in the experimental adhesive (B) when it is polymerized in the presence of 11 wt % water.

## DISCUSSION

The chemistry of the polymeric networks controls the material properties and this relationship is particularly apparent when polymers are used in the wet, oral environment. Monomers that contain polar groups such as carboxylic acid, hydroxyl, amide, ester, urethane, and/or ether linkages are hydrophilic in nature and tend to be more miscible with

water. This is primarily due to the ability of these groups to form hydrogen bonds with water.<sup>8</sup>

Since water or saliva is always present in the mouth of patients during dentin bonding, adhesives should be able to polymerize well in the presence of water or saliva. The new monomer used in this study is a glycerol-based dimethacrylate which contains a branched aromatic ring with a carboxylic acid. Synthesis of the new dimethacrylate monomer is based on the known and frequently applied nucleophilic reaction.<sup>30</sup> We anticipated that the polar nature of the glycerol-based carboxylic acid functional group in this new monomer would lead to a dentin adhesive polymer with improved water miscibility.

Viscosity is of practical importance for dentin adhesives, since less viscous formulations are generally more desirable because of their ease of application and their ability to infiltrate the demineralized dentin matrix. The viscosities of experimental resins were less than those of control resins (Figure 3). These differences are probably due to the lower molecular weight of BMPB and the reduced concentration of the viscous BisGMA in the experimental resins. As expected, the resins formulated with water showed greatly reduced viscosities.

It is generally accepted that the quality of the adhesive bond to dentin is closely related to the infiltration and photopolymerization of adhesive resins. The photopolymerization behavior, that is, the reactivity and DC, plays a very important role in determining the quality of the interfacial hybrid layer. Many studies have shown that conversion of double bonds in the multifunctional methacrylates is rarely complete because the mobility of the propagating free radicals and of the partially and fully polymerized macromolecules is limited as the reaction progresses. Incomplete polymerization can compromise the physical and mechanical properties of resin-based dental restoratives.<sup>8,31</sup> The majority of the light polymerized methacrylate dental resins experience double bond conversion that ranges from 40 to 85%.<sup>32</sup>

The results of this study indicated that the polymerization rate and DC of experimental adhesives were significantly higher than those of the control adhesives (Figures 4 and 5). The improvement in DC afforded by adhesives containing the BMPB is greater when photopolymerized in the presence of water, suggesting better performance in the wet environment of the mouth. This difference in behavior between the experimental and control adhesives may be due to the improved water miscibility of the experimental adhesive. Improved water miscibility may be linked to the relatively hydrophilic nature of BMPB as compared to BisGMA. It was observed that the polymerization rates tended to decrease with the increase of water concentration (Figure 5). In general, the incorporation of water would dilute the concentration of monomers and radicals, so the polymerization rate would decrease.

Since DMA gives information on the relaxation of molecular motions which are sensitive to the structure and variations in the stiffness of materials, it may be used to provide information on the properties of crosslinked polymers, such as storage modulus, glass transition temperature, and structural heterogeneity. In the current study, the adhesive formulated using the newly synthesized monomer, BMPB, when cured in the presence of

water showed storage moduli at 37°C, rubbery moduli, and  $T_g$ s that were significantly greater than the control (Table I). These differences may be related to the higher DC and potentially, improved crosslink density of the experimental adhesives. The rubbery modulus value has been related to the crosslink density of the materials<sup>16,33</sup> and the intensity of the maximal  $\tan \delta$  peak heights reflects the extent of mobility of the polymer chain segments at this temperature.<sup>34</sup> All experimental adhesives cured in the presence of water showed significantly higher rubbery moduli and lower  $\tan \delta$  peak heights than those of the control (Table I), indicating greater crosslink density and increasingly elastic behavior, an implication consistent with the storage moduli and  $T_g$  results. Both the control and experimental adhesives showed reductions in rubbery moduli when cured in the presence of water, suggesting that water may interfere with the formation of crosslinks.

The widths of the  $\tan \delta$  peak (Table I) indicate that the glass transition occurs over a wide temperature range. This broad glass transition can be attributed to heterogeneous networks containing different crosslinked structure regions, resulting in broad distribution of mobilities or relaxation times. The widths of the  $\tan \delta$  peak of experimental adhesives cured in the presence of water are similar to that cured in the absence of water. In contrast, there were substantial differences in the widths of the  $\tan \delta$  peak of control adhesives cured in the presence and absence of water. These results indicate more heterogeneity in the control adhesives cured in the presence of water. The heterogeneity may be related in part to the relatively poor water miscibility of the control adhesives.

The control adhesive could mix with up to 10% water to form a homogeneous solution.<sup>20</sup> The control and experimental adhesives cured in the presence of 10% water were both transparent, without visible voids (unpublished data). However, the microCT images of the control and experimental adhesives cured in the presence of 11% water give a clear comparison of water miscibility. No voids were noted in the microCT images of the experimental adhesive. In comparison, voids were distributed throughout the control adhesive. These differences suggest micro-phase separation of the control adhesive when it is polymerized in the presence of water.<sup>11</sup>

## CONCLUSIONS

A new dimethacrylate monomer with a branched aromatic carboxylic acid group (BMPB) was synthesized by the reaction of phthalic anhydride and GDMA, and used as a co-monomer in dentin adhesives. Adhesives containing BMPB were formulated with the different content of water to simulate the behavior of these materials in the wet, oral environment. The new experimental adhesives showed lower viscosities, and improved monomer/polymer conversion, mechanical properties, and water miscibility as compared to the control adhesives. These results indicate that under conditions simulating the wet, oral environment, BMPB is a feasible co-monomer for dentin adhesives.

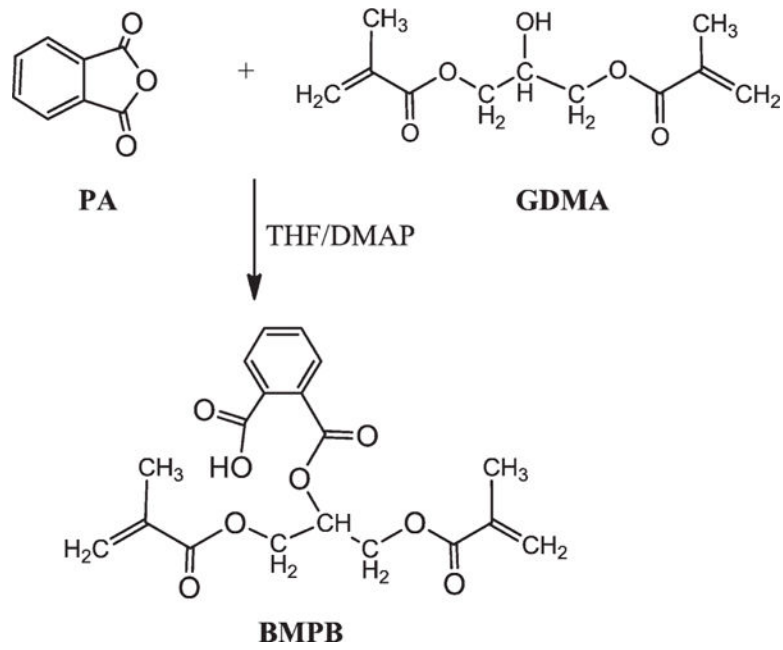
## Acknowledgments

Contract grant sponsor: National Institute of Dental and Craniofacial Research, National Institutes of Health, Bethesda; contract grant numbers: R01DE14392-09, R01DE014392-08S1.

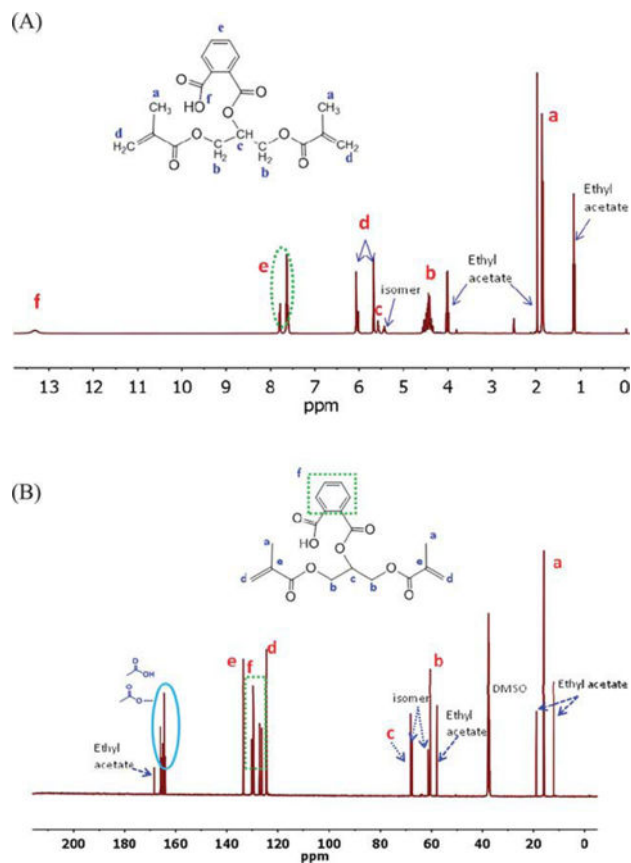
## References

1. Burke F, Wilson N, Cheung S, Mjör I. Influence of patient factors on age of restorations at failure and reasons for their placement and replacement. *J Dent.* 2001; 29:317–324. [PubMed: 11472803]
2. Bernardo M, Luis H, Martin MD, Leroux BG, Rue T, Leitao J, DeRouen TA. Survival and reasons for failure of amalgam versus composite posterior restorations placed in a randomized clinical trial. *J Am Dent Assoc.* 2007; 138:775. [PubMed: 17545266]
3. Levin L, Coval M, Geiger SB. Cross-sectional radiographic survey of amalgam and resin-based composite posterior restorations. *Quintessence Int (Berlin, Germany: 1985).* 2007; 38:511–514.
4. Roulet JF. Benefits and disadvantages of tooth-coloured alternatives to amalgam. *J Dent.* 1997; 25:459–473. [PubMed: 9604577]
5. Murray PE, Windsor LJ, Smyth TW, Hafez AA, Cox CF. Analysis of pulpal reactions to restorative procedures, materials, pulp capping, and future therapies. *Crit Rev Oral Biol Med.* 2002; 13:509–520. [PubMed: 12499243]
6. Ferrari, M., Granik, VT., Imam, A., Nadeau, JC. *Advances in Doublet Mechanics.* Berlin: Springer Verlag; 1997.
7. Hashimoto M, Ohno H, Kaga M, Endo K, Sano H, Oguchi H. Resin-tooth adhesive interfaces after long-term function. *Am J Dent.* 2001; 14:211–215. [PubMed: 11699739]
8. Ferracane JL. Hygroscopic and hydrolytic effects in dental polymer networks. *Dent Mater.* 2006; 22:211–222. [PubMed: 16087225]
9. Wang Y, Spencer P, Hager C, Bohaty B. Comparison of interfacial characteristics of adhesive bonding to superficial versus deep dentin using SEM and staining techniques. *J Dent.* 2006; 34:26–34. [PubMed: 15907359]
10. Ito S, Saito T, Tay FR, Carvalho RM, Yoshiyama M, Pashley DH. Water content and apparent stiffness of non-caries versus caries-affected human dentin. *J Biomed Mater Res B Appl Biomater.* 2005; 72:109–116. [PubMed: 15389491]
11. Spencer P, Wang Y. Adhesive phase separation at the dentin interface under wet bonding conditions. *J Biomed Mater Res A.* 2002; 62:447–456.
12. Spencer P, Wang Y, Bohaty B. Interfacial chemistry of moisture-aged class II composite restorations. *J Biomed Mater Res B Appl Biomater.* 2006; 77:234–240. [PubMed: 16193488]
13. Wang Y, Spencer P. Interfacial chemistry of Class II composite restoration: Structure analysis. *J Biomed Mater Res A.* 2005; 75:580–587. [PubMed: 16104050]
14. Breschi L, Mazzoni A, Ruggeri A, Cadenaro M, Di Lenarda R, De Stefano Dorigo E. Dental adhesion review: Aging and stability of the bonded interface. *Dent Mater.* 2008; 24:90–101. [PubMed: 17442386]
15. Park J, Ye Q, Topp EM, Kostoryz EL, Wang Y, Kieweg SL, Spencer P. Preparation and properties of novel dentin adhesives with esterase resistance. *J Appl Polym Sci.* 2008; 107:3588–3597.
16. Park J, Ye Q, Topp EM, Lee CH, Kostoryz EL, Misra A, Spencer P. Dynamic mechanical analysis and esterase degradation of dentin adhesives containing a branched methacrylate. *J Biomed Mater Res B Appl Biomater.* 2009; 91:61–70. [PubMed: 19358261]
17. Park J, Ye Q, Topp EM, Misra A, Spencer P. Water sorption and dynamic mechanical properties of dentin adhesives with a urethane-based multifunctional methacrylate monomer. *Dent Mater.* 2009; 25:1569–1575. [PubMed: 19709724]
18. Park J, Ye Q, Topp EM, Spencer P. Enzyme-catalyzed hydrolysis of dentin adhesives containing a new urethane-based trimethacrylate monomer. *J Biomed Mater Res B Appl Biomater.* 2009; 91:562–571. [PubMed: 19582843]
19. Ye Q, Wang Y, Williams K, Spencer P. Characterization of photopolymerization of dentin adhesives as a function of light source and irradiance. *J Biomed Mater Res B Appl Biomater.* 2007; 80:440–446. [PubMed: 16850459]
20. Ye Q, Park J, Topp E, Wang Y, Misra A, Spencer P. *In vitro* performance of nano-heterogeneous dentin adhesive. *J Dent Res.* 2008; 87:829. [PubMed: 18719208]

21. Eslick J, Ye Q, Park J, Topp E, Spencer P, Camarda K. A computational molecular design framework for crosslinked polymer networks. *Comput Chem Eng.* 2009; 33:954–963. [PubMed: 23904665]
22. Guo X, Spencer P, Wang Y, Ye Q, Yao X, Williams K. Effects of a solubility enhancer on penetration of hydrophobic component in model adhesives into wet demineralized dentin. *Dent Mater.* 2007; 23:1473–1481. [PubMed: 17316781]
23. Van Landuyt KL, Snauwaert J, De Munck J, Peumans M, Yoshida Y, Poitevin A, Coutinho E, Suzuki K, Lambrechts P, Van Meerbeek B. Systematic review of the chemical composition of contemporary dental adhesives. *Biomaterials.* 2007; 28:3757–3785. [PubMed: 17543382]
24. Moszner N, Salz U. Recent developments of new components for dental adhesives and composites. *Macromol Mater Eng.* 2007; 292:245–271.
25. Podgórski M. Synthesis and characterization of novel dimethacrylates of different chain lengths as possible dental resins. *Dent Mater.* 2010; 26:e188–e194. [PubMed: 20299088]
26. Catel Y, Degrange M, Le Pluart L, Madec P, Pham T, Picton L. Synthesis, photopolymerization and adhesive properties of new hydrolytically stable phosphonic acids for dental applications. *J Polym Sci Part A: Polym Chem.* 2008; 46:7074–7090.
27. Nuti F, Hildenbrand S, Chelli M, Wodarz R, Papini A. Synthesis of DEHP metabolites as biomarkers for GC-MS evaluation of phthalates as endocrine disrupters. *Bioorg Med Chem.* 2005; 13:3461–3465. [PubMed: 15848759]
28. Guo X, Wang Y, Spencer P, Ye Q, Yao X. Effects of water content and initiator composition on photopolymerization of a model BisGMA/HEMA resin. *Dent Mater.* 2008; 24:824–831. [PubMed: 18045679]
29. Park J, Ye Q, Topp EM, Misra A, Kieweg SL, Spencer P. Effect of photoinitiator system and water content on dynamic mechanical properties of a light cured bisGMA/HEMA dental resin. *J Biomed Mater Res Part A.* 2010; 93:1245–1251.
30. Assumption HJ, Mathias LJ. Photopolymerization of urethane dimethacrylates synthesized via a non-isocyanate route. *Polymer.* 2003; 44:5131–5136.
31. Sideridou I, Tserki V, Papanastasiou G. Effect of chemical structure on degree of conversion in light-cured dimethacrylate-based dental resins. *Biomaterials.* 2002; 23:1819–1829. [PubMed: 11950052]
32. Santerre JP, Shajii L, Leung BW. Relation of dental composite formulations to their degradation and the release of hydrolyzed polymeric-resin-derived products. *Crit Rev Oral Biol Med.* 2001; 12:136–151. [PubMed: 11345524]
33. Shi S, Nie J. Investigation of 3, 4 methylenedioxybenzene methoxyl methacrylate as coinitiator and comonomer for dental application. *J Biomed Mater Res B Appl Biomater.* 2007; 82:487–493. [PubMed: 17285604]
34. Hill D, Perera M, Pomery P, Toh H. Dynamic mechanical properties of networks prepared from siloxane modified divinyl benzene pre-polymers. *Polymer.* 2000; 41:9131–9137.



**FIGURE 1.** Reaction scheme for synthesis of 2-((1,3-bis(methacryloyloxy)propan-2-yloxy)carbonyl)benzoic acid (BMPB).

**FIGURE 2.**

<sup>1</sup>H (A) and <sup>13</sup>C (B) NMR spectra in DMSO of new monomer, BMPB. [Color figure can be viewed in the online issue, which is available at [wileyonlinelibrary.com](http://wileyonlinelibrary.com).]

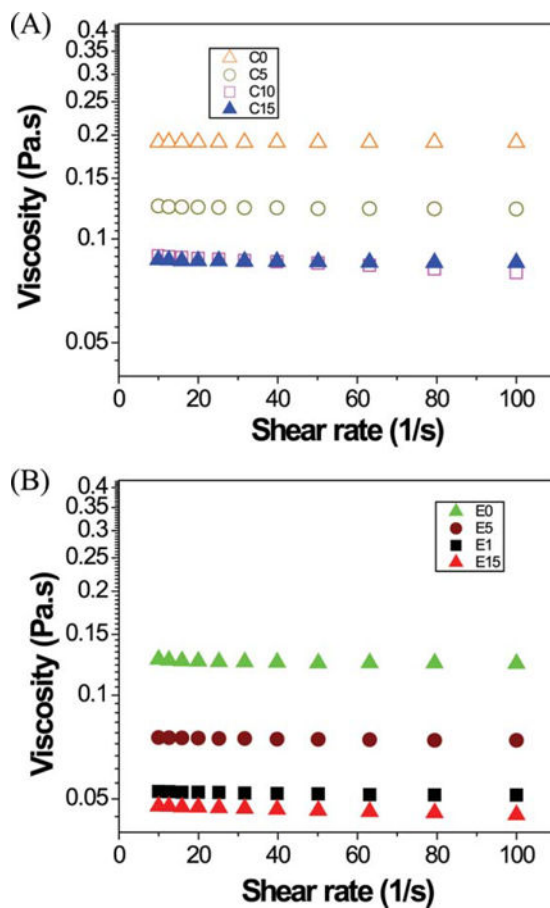


**FIGURE 3.**

The viscosities of control (A: C0, C5, C10, C15) and experimental adhesives (B: E0, E5, E10, E15) as a function of shear rate at 25°C. Control (C): BisGMA/HEMA: 55/45 wt %. Experimental (E): BisGMA/HEMA/BMPB: 30/45/25 wt%. Abbreviations: C, C5, C10, C15 represent control adhesive with 0, 5, 10, 15 wt % water; E, E5, E10, E15 represent experimental adhesive with 0, 5, 10, 15 wt % water. [Color figure can be viewed in the online issue, which is available at [wileyonlinelibrary.com](http://wileyonlinelibrary.com).]

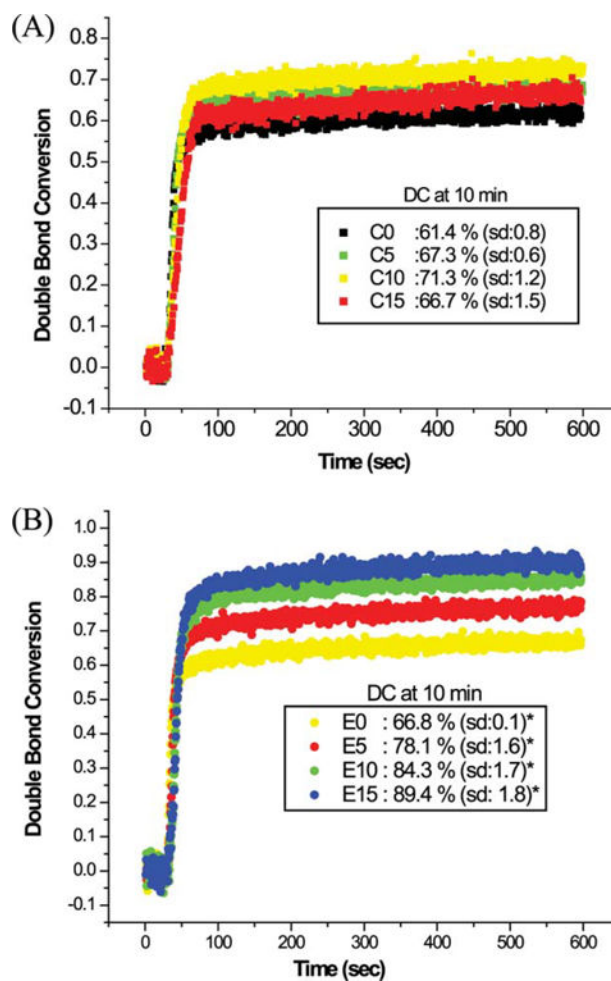


**FIGURE 4.**

Real-time conversion of control (A: C0, C5, C10, C15) and experimental adhesives (B: E0, E5, E10, E15). The adhesives were light-cured for 40 s at room temperature using a commercial visible-light curing unit (Spectrum<sup>®</sup> 800, Dentsply, Milford, DE) at an intensity of 550 mW cm<sup>-2</sup>. \*Significantly ( $p < 0.05$ ) different from the corresponding control. [Color figure can be viewed in the online issue, which is available at [wileyonlinelibrary.com](http://wileyonlinelibrary.com).]

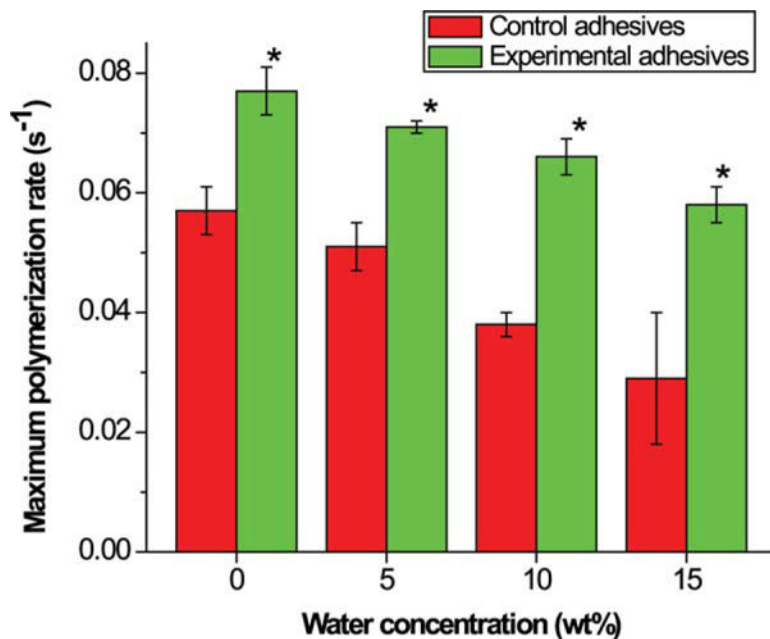


**FIGURE 5.** Maximal polymerization rate of control and experimental adhesives polymerized in the presence of 0, 5, 10, and 15 wt % water.  $N = 3 \pm SD$ . \*Significantly ( $p < 0.05$ ) different from the corresponding control. [Color figure can be viewed in the online issue, which is available at [wileyonlinelibrary.com](http://wileyonlinelibrary.com).]

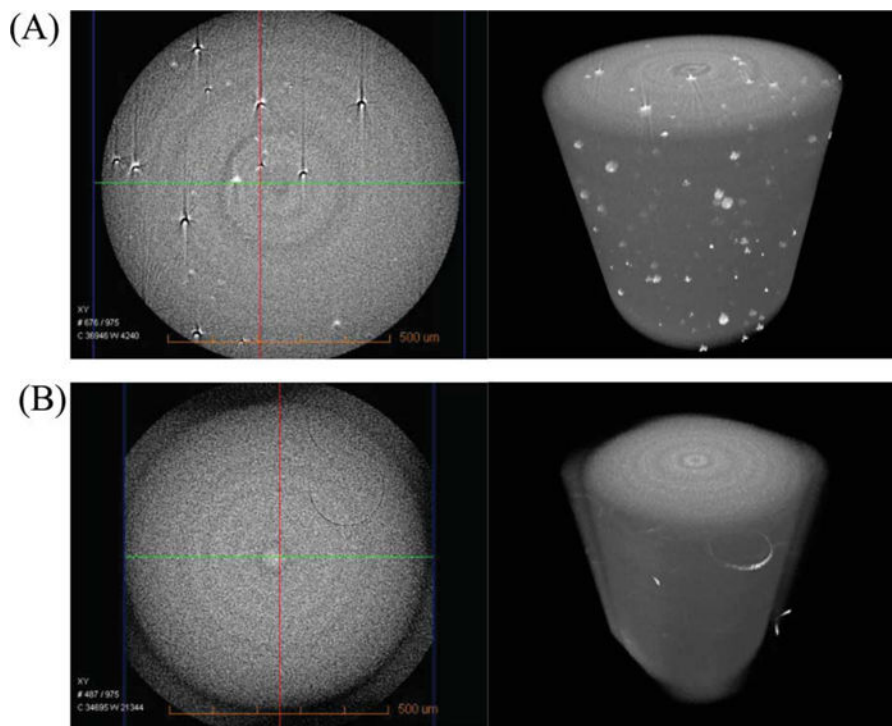


**FIGURE 6.** The microscale morphologies of control (A: the left = CT slice at  $x$ - $y$  plane from 3D image; the right = 3D image) and experimental (B: the left = CT slice at  $x$ - $y$  plane; the right = 3D image) adhesives cured in the presence of 11 wt % water. The morphologies were observed using three-dimensional (3D) MicroXCT (Xradia Inc. Concord, CA). [Color figure can be viewed in the online issue, which is available at [wileyonlinelibrary.com](http://wileyonlinelibrary.com).]

TABLE I

## DMA Data for Control and Experimental Adhesives

Sample	Modulus at 37°C (MPa)	Rubbery modulus (MPa)	$T_g$ (°C)	Height of tan $\delta$ peak	Full-width-at-half-maximum values of tan $\delta$ peak (°C)
C0	3600 (200) <sup>a</sup>	31 (8)	145 (1) <sup>b</sup>	0.67 (0.04)	32.9 (1.0)
C5	3200 (96)	26 (2)	135 (3)	0.75 (0.03)	40.5 (0.6)
C10	2800 (160)	17 (3)	123 (6)	0.72 (0.07)	44.7 (3.3)
C15	2700 (170)	15 (2)	126 (4)	0.79 (0.06)	48.6 (6.3)
E0	4000 (60) <sup>*</sup>	44 (4)	144 (1)	0.62 (0.02)	39.8 (0.9)
E5	3500 (90) <sup>**</sup>	36 (3) <sup>**</sup>	146 (1) <sup>**</sup>	0.64 (0.02) <sup>**</sup>	41.0 (1.5)
E10	3200 (70) <sup>†</sup>	33 (2) <sup>†</sup>	152 (2) <sup>†</sup>	0.65 (0.02) <sup>†</sup>	39.4 (0.5)
E15	3200 (200) <sup>††</sup>	34 (4) <sup>††</sup>	157 (4) <sup>††</sup>	0.63 (0.04) <sup>††</sup>	38.9 (3.1) <sup>††</sup>

<sup>a</sup>Entries are mean values of five specimens with standard deviations in parentheses. Symbols: C0, C5, C10, and C15, control formulations polymerized at 0%, 5%, 10%, and 15% water; E0, E5, E10, and E15, experimental formulations polymerized at 0%, 5%, 10%, and 15% water.

<sup>b</sup>The glass transition temperatures ( $T_g$ ) values of the polymer networks were taken to be the maximum of the tan  $\delta$  versus temperature curve determined using a dynamic mechanical analyzer.

<sup>\*</sup> Significantly ( $p < 0.05$ ) different from control C0;

<sup>\*\*</sup> Significantly ( $p < 0.05$ ) different from control C5;

<sup>†</sup> Significantly ( $p < 0.05$ ) different from control C10;

<sup>††</sup> Significantly ( $p < 0.05$ ) different from control C15.